Finite Elements in Analysis and Design 128 (2017) 19–31

Contents lists available at ScienceDirect

Finite Elements in Analysis and Design

journal homepage: www.elsevier.com/locate/finel

Analysis of experimentally assessed EVA foams with mixed solid-shell elements capable of very large strains

P. Areias[a,b,*], A. Rodrigues[a], T. Rabczuk[c], J. Garção[a], A. Carvalho[a,b,c]

[a] Department of Physics, University of Évora, Colégio Luís António Verney, Rua Romão Ramalho, 59, 7002-554 Évora, Portugal
[b] CERIS/ICIST, Instituto Superior Técnico, Lisboa, Portugal
[c] Institute of Structural Mechanics, Bauhaus-University Weimar, Marienstraße 15, 99423 Weimar, Germany

ARTICLE INFO

Keywords:
Hyperelasticity
Viscoelasticity
Constitutive identification
Strong ellipticity condition
Ogden–Hill
Finite-strain
Solid-shell
Least-squares
Assumed strains

ABSTRACT

We analyze, both experimentally and numerically, two EVA foam specimens with densities $\rho = 120\,\mathrm{kg/m^3}$ and $\rho = 220\,\mathrm{kg/m^3}$. In the numerical analysis, we use our recent finite strain element formulations based on least-squares strains (in both solid-shells and full three-dimensional discretizations). The Ogden–Hill hyperelastic model is coupled with a one-term standard solid containing a Maxwell element. Compression experiments are performed to evaluate the Ogden–Hill properties for the two EVA foams. Viscous properties are obtained from interpolation of creep results reported by R. Verdejo. An exponential integration of the internal variables (which have the role of back-stresses) is proposed along with the complete description of the constitutive system. The classical analysis of the acoustic tensor is also performed for the measured properties. Four benchmark examples are introduced.

1. Introduction

EVA (Ethylene-Vinyl Acetate) foams are adopted in energy-absorbing applications [14,26,33] involving high strain rates. This includes sports applications [26] where EVA foams are typically layered with harder polymers such as polycarbonate [37] or a composite laminate. Polymeric foams damping properties have also been used for sound insulation, cf. [23]. In contrast with other elastomers, EVA foams have excellent fracture toughness. Mechanically, two main ingredients are fundamental in representing the behavior of EVA foams: the elastic non-linearities, traditionally employing the Ogden–Hill model, cf. [27,17] and the viscous behavior which is traditionally based on the standard solid model [39,10,2,12,21]. In EVA foams, the non-linearity is in part due to changes in the microstructural geometry at high strains. The elastic part, consisting of three different stages in compression, is now well understood, cf. [16]. The viscous part is due to air flowing outward of the foam (called gas loss [38]) and requires a specific treatment unlike rubbers (e.g. [24]). For PVC foams, the visco-elastic behavior at high strain rates was studied in detail by Daniel et al., cf. [13]. Elasto-plasticity and failure were investigated by Zhang et al. [40], who proposed a specific yield function for PP, PS and PU foams. The cellular structure of the EVA foam (the case $\rho = 220\,\mathrm{kg/m^3}$) is shown in Fig. 1 where we can observe the closed structure and large variance of cell sizes. A comprehensive treatise on foams is by Gibson and Ashby [16] who discuss in detail the underlying deformation mechanisms at the cell level which explain the macroscopic mechanical behavior.

We present a sufficiently detailed model, as well as the experimental determination of constitutive properties for the EVA foams and the full finite-strain model at high strains and strain rates by combining the Ogden–Hill model with the standard solid. In addition, we use two newly developed elements by our group:

- The finite-strain extension of the Pian/Tong [30], see also [29,34] element introduced by Areias et al., cf. [7].
- The finite-strain solid-shell element by Areias et al. [8].

With some exceptions, foams are usually used only in the compression regime. This poses serious restrictions on the use of EAS and older formulations, see e.g. [6]. In summary, the novelties of this work are:

- The experimental determination of EVA properties by compression tests (performed in a Shimadzu AG-X Plus 100 kN testing machine). Least-squares fitting is used.
- Use of mixed elements capable of very large compressive strains in foam applications without instabilities.
- Introduction of a simplified finite-strain viscoelastic formulation to fit the results of Verdejo [38]. An exponential integrator is used.

* Corresponding author at: Department of Physics, University of Évora, Colégio Luís António Verney, Rua Romão Ramalho, 59, 7002-554 Évora, Portugal.
E-mail address: pmaa@uevora.pt (P. Areias).

http://dx.doi.org/10.1016/j.finel.2017.01.003
Received 19 October 2016; Received in revised form 7 January 2017; Accepted 9 January 2017
Available online 26 January 2017
0168-874X/

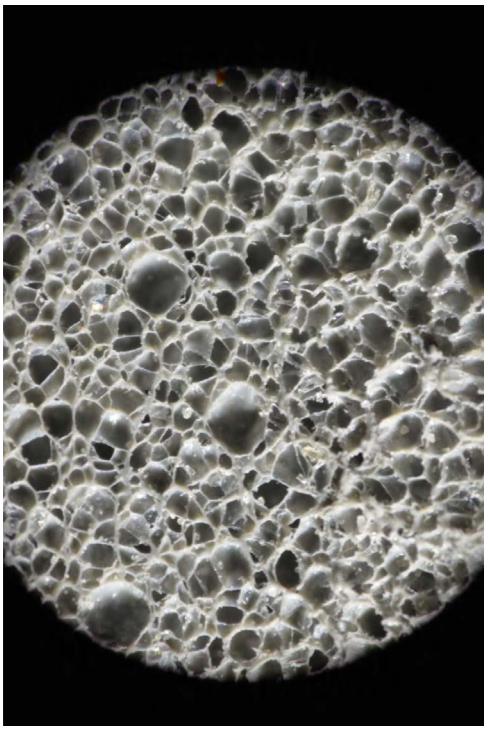

Fig. 1. EVA foam ($\rho = 220\,\text{kg/m}^3$) cellular structure: 9× at the optical microscope, rescaled to fit.

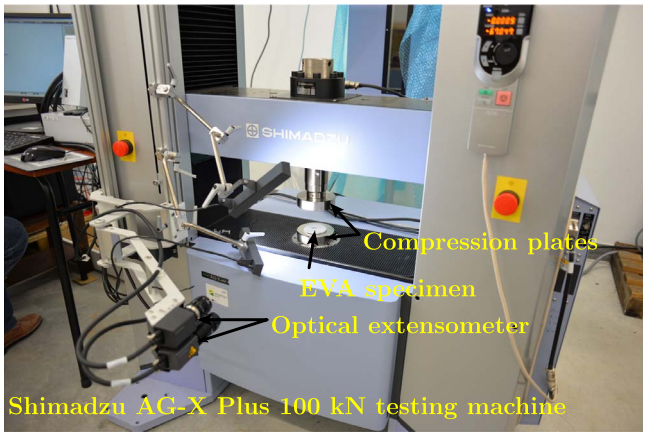

Fig. 2. Compression test of a cylindrical EVA foam.

Table 1
Technical description of the EVA foam specimens.

Specimen	Mass density (kg/m^3) (UNI EN 10902)	Thickness (mm)	Diameter (mm)	Velocity (mm/s)
#1	220	5.25	60	0.1
#2	220	5.25	60	0.5
#3	120	3.1	60	0.1
#4	120	3.1	60	0.5

- The contour maps of the strong ellipticity indicator and the acoustic determinant for the experimentally obtained properties, ensuring well-posedness of the equilibrium problem.
- Four finite-strain benchmarks proposed here for testing of foams.

Table 2
Parameters extracted from [38]: $S_0 = 300 \times 10^3$ Pa, $T = 20$ °C.

Foam ρ (kg/m^3)	ε_0	ε_∞	$E^\star = S/\varepsilon_\infty$ (N/m^2)	γ_∞	τ (s)
108	0.6	0.805	372,671	0.74534	2.08701
146	0.46	0.652	460,123	0.70552	2.12291
151	0.43	0.632	474,684	0.68038	2.15015
152	0.41	0.608	493,421	0.67434	2.15727
265	0.09	0.281	1.0676×10^6	0.32029	3.44251

$S = 300 \times 10^3$ Pa

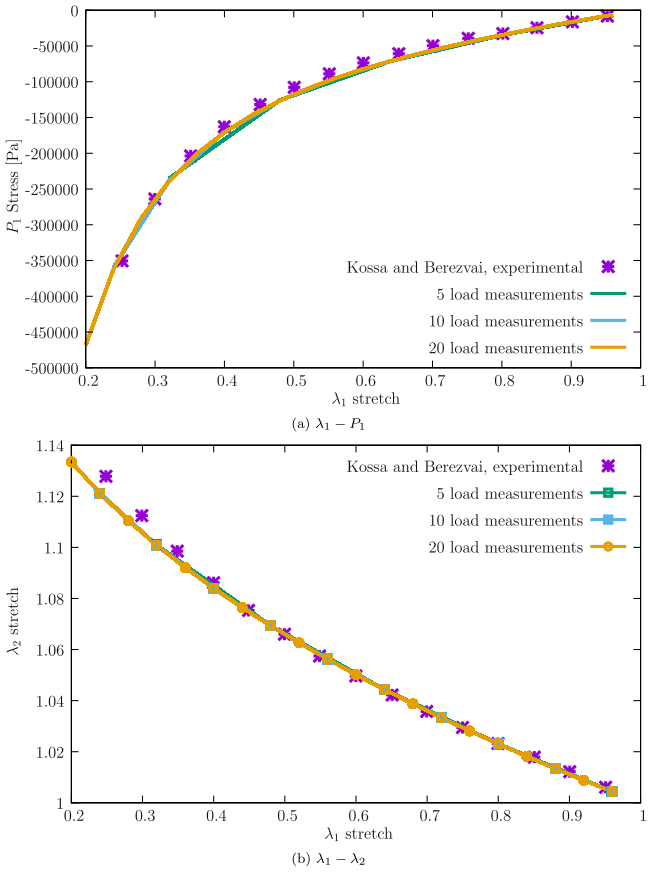

Fig. 3. Comparison with the results by Kossa and Berezvai [20]. Uniaxial loading.

Table 3
Numerically determined properties for the closed-cell polyethylene foam of Kossa and Berezvai.

$\boldsymbol{\alpha}$	$\boldsymbol{\beta}^\star$	$\boldsymbol{\mu}^\star$ (Pa)
$\begin{Bmatrix} 4.14313 \\ 0.13325 \end{Bmatrix}$	$\begin{Bmatrix} 0.078641 \\ 0.078641 \end{Bmatrix}$	$\begin{Bmatrix} 6977 \\ 1.644 \times 10^6 \end{Bmatrix}$

2. Governing equations

We introduce the coordinates of the deformed configuration of a given point X as $\boldsymbol{x}$ and the corresponding undeformed coordinates as $\boldsymbol{X}$. The Cauchy stress tensor is identified by $\boldsymbol{\sigma}$ and second Piola–Kirchhoff stress tensor is identified by $\boldsymbol{S}$. Body forces are identified by $\boldsymbol{b}$. Using the deformation gradient $\boldsymbol{F} = \frac{\partial \boldsymbol{x}}{\partial \boldsymbol{X}}$ and the Jacobian $J = \det \boldsymbol{F}$, a direct manipulation of the equilibrium equations (see e.g. [28]) with the use of the second Piola–Kirchhoff stress, $\boldsymbol{S} = J\boldsymbol{F}^{-1}\boldsymbol{\sigma}\boldsymbol{F}^{-T}$ leads to:

$$\nabla_0 \cdot (\boldsymbol{F}\boldsymbol{S})^T + J\boldsymbol{b} = \boldsymbol{0} \tag{1}$$